Sudan University of Science and Technology

College of Graduate Studies

Modeling and Simulation for Water Sealing Problem In Low Level Sluice Radial Gates At Merowe Dam

نمذجة ومحاكاة مشكلة إنهيار مانع تسرب الماء بأبواب الإطماء بسد مروي

A research submitted in partial fulfillment for the requirements of the degree of M.Sc.in mechatronics engineering

Prepared by:

Mohammed Khalifa Mohammed Alhaj

Supervised:

D. Tawfig Ahmed gamalaldin

May 2018

رَبِّ اجْعَلْنِي مُقِيمَ الصَّلَاةِ وَمِن ذُرِّيَّتِي ۚ رَبَّنَا وَتَقَبَّلْ دُعَاءِ (40)رَبَّنَا اغْفِرْ لِي وَلِوَالِدَيَّ وَلِلْمُؤْمِنِينَ يَوْمَ يَقُومُ الْحِسَابُ(41)

(سورة إبراهيم)

DEDICATION

This research is dedicated for you all:

My mother

My father

My wife & my sons

My brothers & my sisters

ACKNOWLEDGEMENT

My thanks and appreciations to:

Mechanical administration in Merowe dam represented by Eng. M. A. Albagi who provided me with required data.

My colleague Yasir Hassan who provided insight and expertise that greatly assisted the research.

ABSTRACT

The present research discusses a problem of seal damages in dam gates due to influence of water flow through sluices passage way. The low level sluices (L.L.S) of Merowe dam were taken as a research field to investigate the influence of flow on the gate seal. The core of the problem is that the rubbery seal of L.L.S gates is damaged and washed out during yearly operation in flooding season. In previous years there is many solutions has been tried in two ways: first way is by improvement of seal fixture, and the second way is the hydrodynamic approach which focusing on flow behavior in the areas close to the seal. The present study is going through the second approach and a computational fluid dynamic (CFD) software was used to build a model and simulate the water flow through sluice passageway. One of the main result obtained from the study is that the high shear force – as a result of high flow velocity and pressure - subjected on the lower seal is the main cause of the seal damage and it can be reduced by small change in the geometry of that area. The software model results was validated by comparing against instruments measured values and physical observations in the damages area, then finally the research results was concluded and recommendations was introduced.

مستخلص

تناقش هذه الدراسه مشكلة إنهيار وتمزق مانع التسرب في أبواب الخزانات، والناتج عن تأثير تدفق الماء خلال الأبواب. في هذه الدراســـه تم أخذ أبواب الإطماء- أو أبواب المســـتوي الأدني كما تســـمي- بســـد مروي كحقل لإجراء الدراســـه لمعرفة تأثير تدفق الماء علي موانع التسـرب المطاطيه للأبواب. أسـاس وجوهر المشـكله هي ان موانع التسـرب المطاطيه لأبواب الإطماء يحدث لها تمزق وإنجراف عن مجري التثبيت خلال التشغيل السنوي للأبواب في موسم الفيضـــان. في السـنوات الماضـيه تمت محاولة وتجربة عدة حلول لهذه المشـكلة في مسـارين مختلفين: الأول هو تحسين نظام تثبيت مانع التسرب، والمسار الثاني هو المسار الهيدروديناميكي بالتركيز علي دراسة خصـائص السـريان عند منطقة مانع التسـرب. أخذت هذه الدراسه المسـار الثاني وتم عمل نموذج للأبواب بإســـتخدام برامج ديناميكا الموائع التحســـيبيه (CFD) لمحاكاة الســـريان خلال الأبواب. واحده من أهم النتائج المســـتخلصـــه من الدراســـه هي أن قوي القص الكبيره والناتجه عن السرعه والضـغط العاليين عند منطقة مانع التسـرب السـفلي للأبواب تعتبر السـبب الرئيس لتمزق المانع في الجزء السـفلي للأبوب، ويمكن تقليلها بإجراء تعديل بسـيط في الشـــكل الهندســـي للممر في تلك المنطقه. تم التأكد من صـــلاحية النموذج بمقارنته ببعض القيم المقاســـه بأجهزة القياس وبالمقارنه ببعض الملاحظات الفيزيائه في منطقة تمزق مانع التســـرب، كما تم في نهاية البحث ثرد النتائج المستخلصه وتقديم التوصيات اللازمه.

Table of Content

Symbols List

P	Density
ν	Velocity
u, ν, w	Velocity components in x, y, z
L	Length
μ	Dynamic viscosity
ν	Kinematic viscosity
p	Pressure
τ	Shear force
σ	Surface forces
B	Body force
CD	Drag coefficient
A	Area
V	Volume
F	Force
∇	Divergence/gradient operator
Δ	Delta
Q	Heat quantity
E	Internal energy
t	Time
P	Power
g	Gravity acceleration
z	Fluid static head
m	Mass

Appendices List

CHAPTER

INTRODUCTION

1.1 Preliminary

In the field of dams and hydromechanics there are many types of gates used for flow regulation. Spillway gates, bottom gates, power intake gates, and low level sluices gates are the four types of gates used in the project of Merowe dam.

Each type of these gates takes a different form, radial, sliding …etc depending on its function, design capability and operation. And each of them has its own additional emergency repair gates. Low level sluice gates (L.L.S) is the deepest one among other types of the gates, and so named after this characteristic (L.L.S).

The function of L.L.S is to flush the mud sedimentation at flooding season by discharging from the lower level (Lake Bottom).

1.2 Radial gates and sealing mechanism

The flow regulation gate in L.L.S is of type radial. the function of discharge regulation through the L.L.S is conducted by opening and closing the gate completely (no partial opening), and the mechanism of opening-closing is conducted by double acting hydraulic actuator drawing and pushing against the gate arm, and there is a sealing mechanism mounted on the side rail and seal beam of the guide frame.

The mechanism of water sealing mainly depend on rubbery seal which subjected to high pressure through an air bag embedded inside guide frame, receiving its pressurized air from remote air tank and pressing the rubber seal against skin plate of the gate leaf . The rubber seal –which have slight compressibility- clamped and tightened with bolts on the guide frame.

1.3 Problem statement

The root causes of problem of water sealing in L.L.S is that the rubbery seal –which is mounted on the guide frame - is subjected to the forces of flow while fluid

is flowing through the sluice, this result in damage and dislocating of rubbery seal from its groove in the guide frame.

In the yearly checks - (many years) - after flushing season, the rubbery seal was found affected by the water flow in two ways: rubbery seal was damaged and torn up, the second way is that the seal clamp& bolts was untightened and dislocated from their place on the guide frame, so the air bag pulled out and damaged due to strong streaming of the water through sluice passageway.

1.4 Research Objectives

The objective of research is to diagnose the cause and mechanism of seal damage and participate in finding solutions for the water sealing problem and introduce good ideas in the way of studying by focusing the effort on study of the fluid flow characteristics and how it could be changed.

1.5 Scope and limits of the study

1. The study assume that the cause of inflatable rubbery seal fixture removal is due to high vibration induced by vortex of the water flow, and damage of seal is due to force of streaming, so it is focusing only on the flow characteristics.
2. Methods of fixing and mounting the seal are not included in the study
3. There is no real flow model and the study will be conducted with software simulation program (CFD program).
4. The model will be 2D model, so, only upper and lower seal will be included in the study.

1.6 Research methodology

This study following a specified route starting with collecting data related to the gate from construction and O&M manuals, this data includes all drawings of L.L.S water passageway, intake drawing, radial gate drawing and any other drawing related to or involved in the problem. Also data collection includes available data of discharge, pressure head and other flow characteristics.

This data used to determine the type of flow and to building an appropriate software model (using computational fluid dynamics program).The model was built on ANSYS14.0 workbench, and simulation done for the flow characteristics which mainly include: flow velocity, static pressure, total pressure, turbulence K-energy. Then the necessary analysis to reveal the root causes of the problem and give needed recommendations and suggested actions.

Validation of the model was done by comparing to the instruments measured values and to the pictures of damages on the affected areas.

CHAPTER II

THEORATICAL PRINCIPALS & PREVIOUS STUDIES

2.1 Theoretical principal

2.1.1 Types of flow

- Steady flow: in which the fluid characteristics at a point do not change with time
- Uniform flow: in which the velocity at given time does not change with respect to space
- Rotational flow: in which the fluid particles while flowing along streamlines, also rotate about their own axis
- viscous flow: in which the shear force has a considerable value comparing to other forces
- Incompressible flow: in which the changes in density is not considerable.
- Laminar flow: Occurs when the fluid flows in parallel layers, with no mixing between the layers. If we consider a fluid flow inside a cylindrical pipe, the fluid layer flow at the center is the fastest, and the cylinder touching the pipe isn't moving at all.

  The flow is considered laminar when Reynolds number (Re) is less than 2300

- Turbulent flow: the turbulent flow occurs when the liquid is moving fast with mixing between layers. The speed of the fluid at a point is continuously undergoing changes in both magnitude and direction.

  The flow is considered turbulent when Reynolds number is greater than 4000

- Transitional flow: Transitional flow is a mixture of laminar and turbulent flow, with turbulence flow in the center of the pipe and laminar flow near the edges of the pipe. Each of these flows behaves in different manners in terms of their frictional energy loss while flowing and have different equations that predict their behavior.

  The flow is transitional when Reynolds number is in between 2300 and 4000

$$\mathrm{Re} = \frac{\rho u L}{\mu} = \frac{u L}{\nu}$$ (1) (M.Hashim Siddig, 2006)".

- Dimensions of flow: the flow is described as one, two, three dimensions corresponding to the minimum number of co-ordinates describing the flow.
- Body forces& surfaces forces: body force is the force induced by the body mass such as gravitational force. And surface force is the force on the body surface which include only shear and pressure forces.

Surface force: $\sigma = -pn + \tau$

For fluid flow, the Drag force: $$F_D = \frac{1}{2} \rho v^2 C_D A$$ (2) (M.Hashim Siddig, 2006)".

2.1.2 Some fluid flow phenomenons

- **Separation**

Flow separation is boundary layer separation and it occurs whenever the change in velocity of the fluid -in either magnitude or direction- is too large for the fluid to adhere to the solid surface. Or it is a reversing of the velocity direction inside the boundary layer of the flow due to existence of positive pressure gradient in the flow direction, the velocity distribution in specified point decreases to zero and then reverse the flow direction and the fluid start to rotate locally as illustrated in fig.2.1 bellow (M.Hashim Siddig, 2006)".

So, Flow separation occurs when:

1/ the velocity at the wall is zero or negative and an Inflection point exists in the velocity profile

2/ and a positive or adverse pressure gradient occurs in the direction of flow

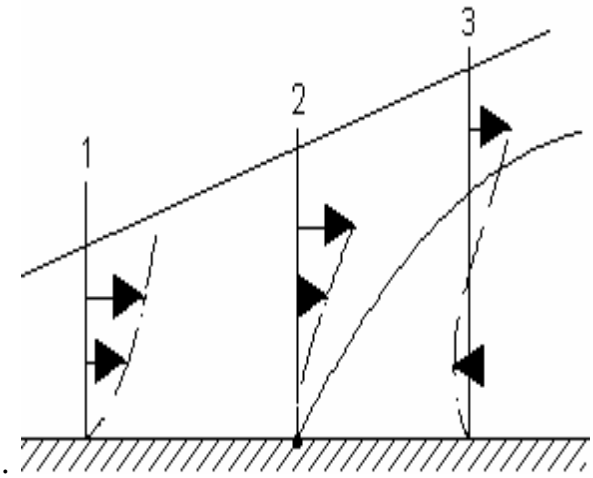

Figure 2.1: reverse of flow direction inside boundary layer

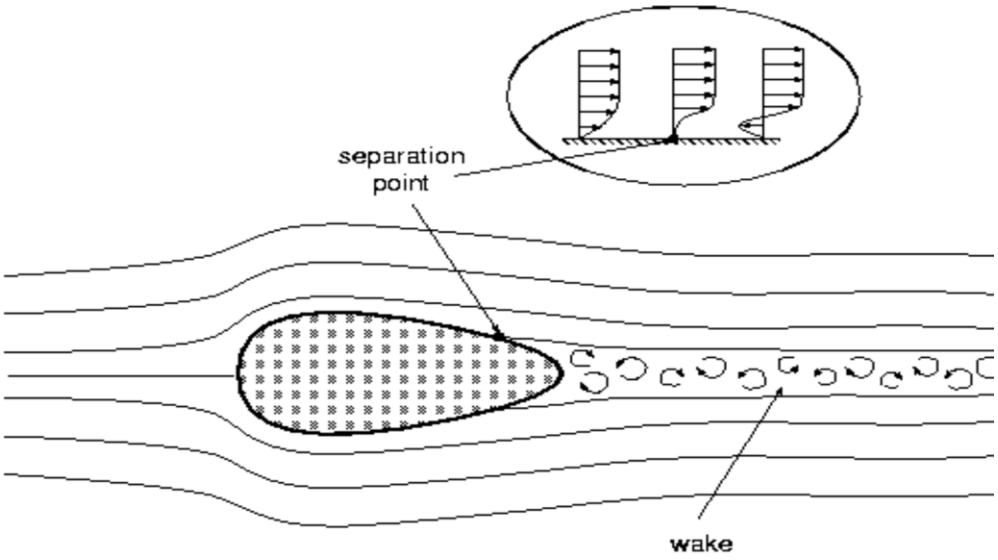

Figure 2.2: separation of flow

- **Cavitation**

Cavitation is the formation of vapour cavities in a liquid, (bubbles" or "voids).it is a multiphase phenomenon including vapor bubbles creation and collapse occurring alternately at high frequency in liquid stream (Dorota Homa, 2017) ” . It usually occurs when a liquid is subjected to rapid changes of pressure “for example during acceleration of the liquid”. When the liquid subjected to higher pressure, the voids

implode and can generate an intense pressure shock wave, which spread through the flow.

When pressure declines, the gas nuclei in the flow start to grow. The phase change is observed, like during the boiling process, but the driving mechanism is different, in boiling process it is temperature changes, in cavitation it is pressure changes. The phase diagram of water is shown in Fig.2.3 below. The cavitation process is represented by the vertical line; with the assumption the global temperature during the process is constant. Pressure changes are dependent on dynamics of flow, according to Bernoulli's equation (3), where no energy losses are assumed.

$$\frac{p}{\rho} + \frac{v^2}{2} = const \qquad (3)$$

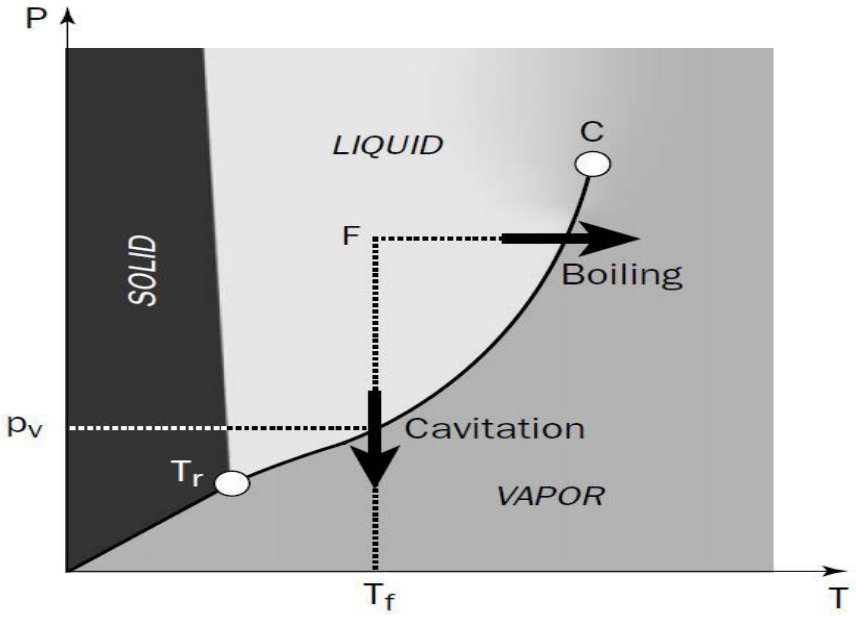

Figure 1.3: phase diagram of water

Cavitation is a significant cause of wear in some engineering contexts. Collapsing voids that implode near to a metal surface cause cyclic stress through repeated implosion. These results in surface fatigue of the metal causing a type of wear also called "cavitation.

2.1.3 Governing equation of fluid flow

The governing equation of fluid flow is based and derived of conservation laws: mass conservation, energy conservation and conservation of momentum.

Mass conservation law

The principle that in any closed system, the mass is constant irrespective of its changes in form. Or, mass is neither created nor destroyed.

This Principle is applied to a fixed volume in space of arbitrary shape that contains fluid; this volume is called a "Control Volume." Fluid is permitted to enter or leave the control volume. A control volume $\forbar{V}$ is shown in the sketch bellow

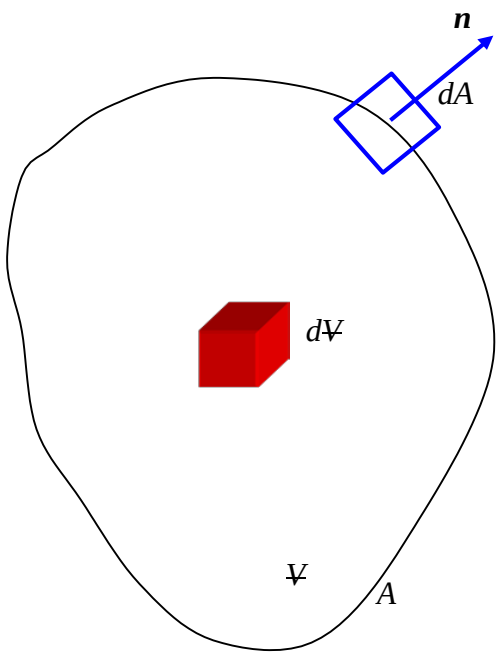

[Rate of increase of mass of material within the control volume = Net rate at which material enters the control volume.] (R. Shankar Subramanian) ".

$$\oiiint \frac{\partial \rho}{\partial t} dV = - \oiint \rho V . dA \qquad (4)$$

For incompressible, steady, two directional flow, the above equation can be adapted to:

$$\rho VA = const \qquad (5)$$

This equation in its differential form called: *continuity equation*

$$\frac{\partial \rho}{\partial t} + \frac{\partial u}{\partial x} + \frac{\partial v}{\partial y} + \frac{\partial w}{\partial z} = 0 \qquad (6)$$

Energy conservation low

The principle of conservation of energy for a control mass system is described by the first law of thermodynamics:

[Heat Q added to a control mass system + the work done W by the control mass system = change in its energy E**]**

Or it can be written:

'[Heat Q added to a control mass system + the work done W by the control system = Rate of increase of energy within the control volume + Net rate at which energy leave the control volume]

$$\iiint \frac{\partial \rho}{\partial t}\left[\rho\left(e + \frac{v^2}{2} + gz\right)\right] dV + \oiint \rho\left(e + \frac{v^2}{2} + gz\right)\underline{v}.\, d\underline{A} = -\oiint p\underline{v}.\, d\underline{A} + P + \dot{Q}$$

(7)

For inviscid, incompressible, steady, one dimensional flow and neglecting change in temperature and heat transfer, the energy equation adapted to:

$$\frac{p_1}{\rho_1 g} + \frac{{v_1}^2}{2g} + z_1 + \frac{P}{\dot{m} g} = \frac{p_2}{\rho_2 g} + \frac{{v_2}^2}{2g} + z_2 \qquad \textbf{(8)}$$

Momentum conservation low

Starting from Newton's second low of motion we can write:

[The rate of change of momentum of a body is equal to the resultant force acting on the body, and takes place in the direction of the force.]

$$\iiint \frac{\partial}{\partial t}(\rho \underline{v})dV + \oiint \rho \underline{v}(\underline{v}.\, d\underline{A}) = \iiint \underline{B}\, dV + \oiint \underline{\sigma} dA \qquad (9)$$

2.1.4 Modeling and simulation of physical processes

1. defining the physical problem
2. creation of a mathematical model(PDE)
    - systems of PDEs, ODEs, algebraic equations
    - defining initial and boundary conditions
3. creation of a discrete (numerical) model
    - discretize the domain and generate the grid
    - solve the discrete model
4. analyzing errors in the discrete system
    - doing the consistency, stability and convergence analysis

- In the next two sections the focus will be on the second and third points which concerning with the mathematical model and its solution.

2.1.5 Navier-Stokes Equations

The present mathematical model is based mainly on Navier-Stokes (PDE) Equations

Navier-Stokes equations derived from equation of momentum conservation (9) in its differential form.

Surface integral converted to volume integral by using **Divergence Theorem:**

$$\iiint_V (\nabla . \mathrm{F})\, dV = \oiint_A (\mathrm{F} . \mathrm{n})\, dA \qquad (10)$$

Then we obtain the three equation of three dimensions flow (Navier-Stokes equation).

$$\rho\left[\frac{\partial u}{\partial t} + u\frac{\partial u}{\partial x} + v\frac{\partial u}{\partial y} + w\frac{\partial u}{\partial z}\right] = B_x - \frac{\partial p}{\partial x} + s_x$$

$$\rho\left[\frac{\partial v}{\partial t} + u\frac{\partial v}{\partial x} + v\frac{\partial v}{\partial y} + w\frac{\partial v}{\partial z}\right] = B_y - \frac{\partial p}{\partial y} + s_y \ldots$$

$$\rho\left[\frac{\partial w}{\partial t} + u\frac{\partial w}{\partial x} + v\frac{\partial w}{\partial y} + w\frac{\partial w}{\partial z}\right] = B_z - \frac{\partial p}{\partial z} + s_z \ldots$$

Where: u, v, w, is the velocity component in the x, y, z, directions. And $S_{x,y,z,}$ is the shear stress components in x, y, z, directions.

- Stokes subtracts the values of **S** as below:

$$s_x = \frac{\partial}{\partial x}\left\{\mu\left[2\frac{\partial u}{\partial x} - \tfrac{2}{3}\left(\frac{\partial u}{\partial x} + \frac{\partial v}{\partial y} + \frac{\partial w}{\partial z}\right)\right]\right\} + \frac{\partial}{\partial y}\left\{\mu\left[\frac{\partial u}{\partial y} + \frac{\partial v}{\partial x}\right]\right\} + \frac{\partial}{\partial z}\left\{\mu\left[\frac{\partial w}{\partial x} + \frac{\partial u}{\partial z}\right]\right\}$$

$$s_y = \frac{\partial}{\partial y}\left\{\mu\left[2\frac{\partial v}{\partial y} - \tfrac{2}{3}\left(\frac{\partial u}{\partial x} + \frac{\partial v}{\partial y} + \frac{\partial w}{\partial z}\right)\right]\right\} + \frac{\partial}{\partial z}\left\{\mu\left[\frac{\partial v}{\partial z} + \frac{\partial w}{\partial y}\right]\right\} + \frac{\partial}{\partial x}\left\{\mu\left[\frac{\partial u}{\partial y} + \frac{\partial v}{\partial x}\right]\right\}$$

$$s_z = \frac{\partial}{\partial z}\left\{\mu\left[2\frac{\partial w}{\partial z} - \tfrac{2}{3}\left(\frac{\partial u}{\partial x} + \frac{\partial v}{\partial y} + \frac{\partial w}{\partial z}\right)\right]\right\} + \frac{\partial}{\partial x}\left\{\mu\left[\frac{\partial w}{\partial x} + \frac{\partial u}{\partial z}\right]\right\} + \frac{\partial}{\partial y}\left\{\mu\left[\frac{\partial v}{\partial z} + \frac{\partial w}{\partial y}\right]\right\}$$

For inviscid flow the term S in the equation is equal to zero, and the equations in this case called Euler equations.

Navier-Stokes equations are partial differential equations, so, in most cases there is no exact solution for it due to nonlinearity of some terms of the equation (M.Hashim Siddig, 2006)".

In practical applications of problems modeling it was resorted to numerical solutions which are approximate solutions.

2.1.6 Numerical methods of solution of partial differential equations (PDEs)

- The Finite Difference Method (FDM)
- The Finite element Method (FEM)
- The Finite volume Method (FVM)

The Finite Difference Method (FDM)

This method is used to obtain numerical approximations of PDEs written in the strong form. The derivative of u(x) with respect to x can be defined as:

$$u_x(x_i) = \lim_{\Delta x \to 0} \frac{u(x_i + \Delta x) - u(x_i)}{\Delta x}$$

If Δx is small but finite we can use the approximation:

$$u_x(x_i) \approx \frac{u_{i+1} - u_i}{\Delta x}$$

The analysis of these approximations is performed by using Taylor expansions around the point xi

$$u_{i+1} = u_i + u_x|_i \, \Delta x + u_{xx}|_i \frac{\Delta x^2}{2} + \cdots + \left.\frac{\mathrm{d}^n u}{\mathrm{d}x^n}\right|_i \frac{\Delta x^n}{n!} + \underline{\frac{\mathrm{d}^{n+1} u}{\mathrm{d}x^{n+1}}(x^*)\frac{\Delta x^{n+1}}{(n+1)!}}.$$

The underlined term is called the remainder with xi ≤ x ≤ xi+1, and represents the error in the approximation if only the first n terms are kept.

Although the expression is exact, the position x^* is unknown.

For n= 1:

$$\frac{u_{i+1} - u_i}{\Delta x} = u_x|_i + \frac{\Delta x}{2} u_{xx}(x^*).$$

OR

$$u_x(x_i) = \frac{u_{i+1} - u_i}{\Delta x} + \epsilon_T$$

The term ϵ_T is referred to as the truncation error and is defined as the difference between the exact value and its numerical approximation. This term not only depends on Δx but also on u and its derivatives. For instance, if u(x) is a linear function then the finite difference approximation is exact and ϵ_T = 0 since the second derivative is zero.

The solution is obtained by substituting the boundary conditions on the discrete form to get a linear system of N equations with N unknowns which can be solved directly by first or second order discretization (Joaquim Perio, Spencer Sherwin, 2005)".

Consider the equation u_{xx} = s(x) in the region Ω = {*x:* 0 ≤ *x* ≤ 1}.

Discretizing the region using *N* points with constant mesh spacing Δ*x* = *(1/N−1)* or *xi =(i − 1/N− 1)*, we consider two cases with different sets of boundary conditions:

1. u(0) = α_1 and u(1) = α_2

2. u(0)= α_1 and $u_x(1)$ = *g*.

- The first case is straightforward by direct substitution of the boundary conditions $u_1 = \alpha_1$ and $u_n = \alpha_2$

These two conditions together with the N −2 equations result in the linear system of N equations with N unknowns represented by the matrix:

$$\begin{bmatrix} 1 & 0 & & \dots & & & 0 \\ 1 & -2 & 1 & 0 & \dots & & 0 \\ 0 & 1 & -2 & 1 & 0 & \dots & 0 \\ & & \ddots & \ddots & \ddots & & \\ 0 & \dots & 0 & 1 & -2 & 1 & 0 \\ 0 & & \dots & 0 & 1 & -2 & 1 \\ 0 & & & \dots & & 0 & 1 \end{bmatrix} \begin{bmatrix} u_1 \\ u_2 \\ u_3 \\ \vdots \\ u_{N-2} \\ u_{N-1} \\ u_N \end{bmatrix} = \begin{bmatrix} \alpha_1 \\ \Delta x^2 s_2 \\ \Delta x^2 s_3 \\ \vdots \\ \Delta x^2 s_{N-2} \\ \Delta x^2 s_{N-1} \\ \alpha_2 \end{bmatrix}$$

- In the second case if we use the approximation

$$u_x(1) \approx \frac{u_N - u_{N-1}}{\Delta x} = g.$$

The error could potentially reduce the global accuracy of the solution, so the alternate solution is to use a second-order centered approximation (discretization) which more accurate than first-order discretization.

$$u_x(1) \approx \frac{u_{N+1} - u_{N-1}}{2\Delta x} = g$$

The value $u_{N+1}$is not available since it is not part of our discrete set of values but we could use the finite difference approximation at x_N given by

$$\frac{u_{N+1} - 2u_N + u_{N-1}}{\Delta x^2} = s_N$$

Where $s_N = u_{xx}(N)$

So we obtain

$$u_N - u_{N-1} = (g\Delta x - \frac{1}{2} s_N \Delta x^2)$$

The Finite element & Finite volume Method (FEM & FVM)

Beside FDM method, which uses the strong or differential form of the governing equations, there are two other alternative methods use the integral form of the equations which have more advantages over the differential form as no requirement of continuity, natural treatment of boundary conditions and suitable for dealing with complex geometry due to independence of mesh structure.

These alternative methods are: finite element FEM and finite volume FVM methods.

The final expression of these two methods respectively is:

$$-\frac{u_i - u_{i-1}}{\Delta x_{i-1}} + \frac{u_{i+1} - u_i}{\Delta x_i} = \frac{\Delta x_{i-1} + \Delta x_i}{2} s_i.$$

$$u_t|_i \left(x_{i+(1/2)} - x_{i-(1/2)}\right) + f\left(u_{i+(1/2)}\right) - f\left(u_{i-(1/2)}\right) = 0.$$

2.2 Previous studies

There are many studies and papers established in the field of dam gates sealing, and in the field of flow modeling such as:

1/ Bottom outlet dam flow: physical and numerical modelling

By:- Farhang Daneshmand PhD

Adjunct Associate Professor, Department of Bioresource Engineering, McGill University, Ste. Anne deBellevue, Canada; Associate Professor, Faculty of Mechanical Engineering, Shiraz University, Shiraz, Iran

-Jan Adamowski MPhil, MBA, PhD Assistant Professor, Department of Bioresource Engineering, McGill University, Ste. Anne de Bellevue, Canada

-Tahereh Liaghat MSc Graduate Student, Mechanical Engineering Department, E´ cole Polytechnique de Montre´ al, Montre´ al, Canada

This paper presents an analysis of flow parameters through a bottom outlet conduit with gated operation using physical and numerical models. A physical model of the regulating bottom outlet of Shahryar dam in Iran was used to investigate the hydraulic forces on the service radial gate and flow patterns within the conduit. The model was constructed from Plexiglas, and discharge and pressure data were recorded for different gate openings. The Froude law of similarity was satisfied in the hydraulic modelling, allowing for an investigation of the dynamic similarity of inertial and gravitational forces. The numerical scheme was based on using the natural-element method to study hydraulic forces and flow parameters within the conduit and the finite-element method to evaluate the natural frequencies of the radial gate. The results of the calculations for different radial gate openings showed good agreement with those from physical modelling for the pressure distributions throughout the flow.

The paper conclude to that With rapidly changing, in numerical modelling, engineers have the possibility of using combined physical and computational methods in the design and analysis of hydraulic structures and conduits. A combined physical and numerical method was presented in this paper. The physical model was based on the Froude similarity criteria, whereas the numerical analysis was performed using NEMs and FEMs. The results of a hydraulic model test of the bottom outlet of

Shahryar dam in Iran were presented. The main results of the hydraulic test were gate discharge characteristics, gate loading and the shape of water passage, which did not include zones of low pressure with high cavitation potential. The measured values of pressure were used to evaluate the hydrodynamic forces and force coefficients. A computational procedure based on the NEM was used to predict the free-surface profile of the flow under the emergency gate and the velocity contour in the channel. The dynamic characteristics of the radial gate of Shahryar dam were studied in the hydraulic model test. Pressure fluctuations induced by turbulence on the skin plate at different local openings, which is the basic dynamic load acting on the gates, were also investigated. The FEM was also used to analyze the free vibration characteristics of the radial gate at different openings. The measurements showed that the pressure fluctuations in the present case were random in the time domain. Moreover, the results obtained from the hydraulic model test showed that the fundamental frequency of the service radial gate was sufficiently far from the dominant frequencies in the power spectral density of the pressure fluctuations and therefore the gate is free from the risk of resonance. There was reasonably good agreement between the physical and numerical models.

2/ Numerical Modeling of Flow over an Ogee Crested Spillway under Radial Gate: VOF and MMF Model.

By: Date V1, Dey T and Joshi

1. Department of Mechanical Engineering, D.Y. Patil College of Engineering, Akurdi, Pune 411044; Savitribai Phule Pune University, Pune, India

2. Water Resource Department, Dapodi, Pune, India

This research work shows the simulation of the gated flow over an ogee crested spillway for one of water reservoir. The average velocities and Froude Number analysis at various gate openings gives a better insight of flow behavior. Also, the simulations were carried out by changing the gate bottom shape. The STAR CCM+ CFD tool is used to solve the fluid flow performance. The flow parameters near the bottom of the gate have been studied with two types of fluid flow models i.e. Volume

of Fluid (VOF) and Multi-Mixture Fluid Models. The use of Volume of Fluid (VOF) multiphase model together with RNG k-ε turbulence for the simulation, gives the excellent agreement between the experimental and numerical data. The spillway performance of the gated flow at various gate openings resembles with the actual flow behavior. The applicability of the CFD model to simulate the gated flow over ogee crested spillway is reviewed. The computational model study showed that CFD can be useful in hydraulics structures for designing of various reservoirs. This numerical model gives significant advantage in practice, in terms of parametric studies.

The study conclude that the numerical model using VOF multiphase flow model together with RNG k-ε turbulence model is more suitable than MMF model to simulate the flow over an ogee crested spillway with gated flow. The data obtained from large scale experiments of dam reservoir verifies the VOF model data more significantly. The Froude Number variation after 1m gate opening approaches towards unity i.e. flow tends to be critical. So we must not keep the open at 1m opening for long time as the flow is more supercritical in this region it should be operated at 6`m or full gate opening for dam reservoir. This study showed that CFD can be viewed as better design tool for hydraulic structures with proper analysis for validation.

Number of cases could be easily simulated which provide us the information about the various flow parameters such as velocity, flow, pressure, and another parameter associated with dam flow. Finally, the numerical model has many advantages in practice, in terms of parametric study.

3/ Numerical flow simulation in gated hydraulic structures using smoothed fixed grid finite element method.

By: Mohammad Javad Kazemzadeh-Parsi

Young Researchers and Elite Club, Shiraz Branch, Islamic Azad University, Shiraz, Iran

The abstract of this paper is that a Successful design and operation of hydraulic structures require more effective and reliable tools to be used in a variety of practical problems, including bottom outlets, intakes and/or spillways. Until recently, physical modeling has been the principal approach in studying the flow pattern and behavior of

such structures. The main concerns might generally be related to estimating of discharge coefficients, frictional losses, details of local flow patterns, position of the free surface, and air entrainment. The application of a new developed numerical modeling for free surface flow simulation in gated tunnels is presented here.

Among various parameters, the free surface profile, pressure distribution and discharge of the flow passing through gated hydraulic structures are considered in the present study. The solution of free surface flow problems is usually carried out through an iterative process due to unknown geometry and nonlinear boundary conditions. Therefore, the solution of these problems using traditional numerical methods presents some difficulties since the computational mesh needs to be modified for each iteration. The application of the smoothed fixed grid finite element method in the solution of free surface flow problems is investigated in this paper. The main advantage of the proposed method is that it is based on non-boundary-fitted meshes which simplify the solution procedure. In this method, the gradient smoothing technique is used to facilitate formulation of boundary intersecting elements. To evaluate the applicability of the proposed method, three representative examples are solved and the results are compared with experimental and numerical results available in the literature. The results of the present study indicated the power of smoothed fixed grid finite element method in solving the free surface potential flows through gated hydraulic structures.

The smoothed fixed grid finite element method is used to solve free surface potential flow problems. In this method, a fixed non-boundary-fitted mesh is used to solve the governing equation and to obtain the field variable. The main motivation for the use of non-boundary-fitted meshes in the solution of variable domain problems is that there is no need to modify the mesh in each iteration. In this method, the gradient smoothing technique is used to obtain gradients of the field variables and this causes the domain integrals to reduce to line integrals on the edges of the smoothing cells. This significantly simplifies computation of the matrices of the boundary intersecting elements. To evaluate the applicability of the proposed method three example problems were solved. In the first example, the flow under a sluice gate was considered for different gate openings and the results were compared with other numerical results available in the literature. In the second example, the flow under a radial gate located over a spillway was considered and the results were compared with an experimental correlation. In the last example, a bottom outlet was considered and the results were

compared with results of a hydraulic scaled model test. The results demonstrate that the smoothed fixed grid finite element method can effectively be used in the solution of free surface potential flow problems in the gated hydraulic structures.

4/ Program of the Hydraulic and Flow-Induced Vibration Model Test for Low-Level Sluices Working Gate (Merowe dam)

By: College of Water Resources and Hydropower, State Key Laboratory of Water Resources and Hydropower Engineering Science, Wuhan University, China October, 2011,

Which conclude that the bottom flow condition is complex, there is a big negative pressure area, air supply to the bottom sill is not satisfactory. In order to solve those problems, hydraulics model test and flow induced vibration model test are made to test the gate slot and adjacent areas cavitation condition, and to put forward improvement and optimization measures for air supply to the bottom sill to solve the problem of the bottom air supply inadequacy, charging pressure, water seal vibration and cavitation. Also they recommend to construct a concrete jump behind seal area to buildup pressure.

CHAPTER III

RESEARCH METHODOLOGY

3.1 Core of the study

The core of the present study is to build a software model to simulate the flow of water through the sluice and then validate the built model by comparing against empirical and measured data's, and finally extract the causes of seal damage and prove the validity of the assumed causes.

Before going through the model, the flow will be defined as steady flow, so there are no concerns about the transient stage (mainly while gate opening and closing), but -in contrast- the behavior of flow in the transient stage will be used as additional confirmation of results validation.

Also from the average of yearly measured value of flow velocity through sluice passageway (24.7m/s) and characteristics of water at $25c^{o}$, the Reynold's number = $\mathbf{94E^{6}}$ so it was clearly a fully turbulent flow.

3.2 Turbulence modeling

Turbulent flows are characterized by fluctuating velocity fields. These fluctuations mix transported quantities such as momentum, energy, and species concentration, and cause the transported quantities to fluctuate as well. Since these fluctuations can be of small scale and high frequency, they are too computationally expensive to simulate directly in engineering calculations. Instead, the instantaneous (exact) governing equations can be time-averaged, or otherwise manipulated to remove the small scales, resulting in a modified set of equations that are computationally less expensive to solve. However, the modified equations contain additional unknown variables, and so turbulence models are needed to determine these variables in terms of known quantities.

Turbulence models

Because of the fact that the turbulence is a random process, it is not applicable to 'perfectly' represent the effects of turbulence in the CFD simulation. Instead the Turbulence Models is needed.

These models is a simulation tools and we have to pick the most appropriate tools of them to suit our simulations.

It is an unfortunate fact that no single turbulence model is universally accepted as being superior for all classes of problems. The choice of turbulence model will depend on considerations such as the physics encompassed in the flow, the established practice for a specific class of problem, the level of accuracy required, the available computational resources، and the amount of time available for the simulation. To make the most appropriate choice of model for the present application, there is a need to understand the capabilities and limitations of the various options.

Here the discussion will be only for the models included in the used CFD software (ANSYS- FLUENT).

In fluent there are main two categories of turbulent models which have its own sub models.

- Large Eddy Simulation (LES).
- Reynolds-Averaged Navier Stokes (RANS).

3.2.1 Large Eddy Simulation (LES)

In LES the large eddies are computed in a time-dependent simulation that uses a set of filtered equations. Filtering is essentially a manipulation of the exact Navier-Stokes equations to remove only the eddies that are smaller than the size of the filter, which is usually taken as the mesh size. Like Reynolds averaging، the filtering process creates additional unknown terms that must be modeled in order to achieve closure, (Closure implies that there are a sufficient number of equations for all the unknowns).

Statistics of the mean flow quantities، which are generally of most engineering interest, are gathered during the time-dependent simulation. The attraction of LES is that, by modeling less of the turbulence (and solving more), the error induced by the turbulence model will be reduced.

3.2.2 Reynolds-Averaged Navier Stokes (RANS)

This is the main tool used by engineers. In which the equations are solved for time-averaged flow behavior and the magnitude of turbulent fluctuations.

The approach of permitting a solution for the mean flow variables greatly reduces the computational effort. If the mean flow is steady (ANSYS customer training material, 2010) the governing equations will not contain time derivatives and a steady-state solution can be obtained economically. A computational advantage is seen even in transient situations, since the time step will be determined by the global unsteadiness in the mean flow rather than by the turbulence.

Mean and Instantaneous variables.

In Reynolds averaging, the solution variables in the instantaneous (exact) Navier-Stokes equations are decomposed into the mean (ensemble averaged or time-averaged) and fluctuating (in three directions) components

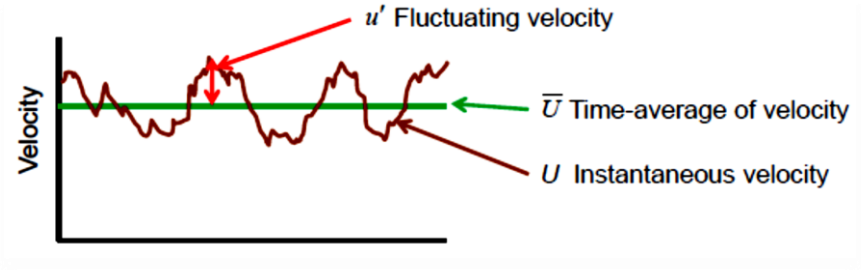

Figure 2.1: components of turbulent velocity.

If we recorded the velocity (and other variable) at a particular point in the real (turbulent) fluid flow, the instantaneous variables would look like this:

$$u_i = \overline{u_i} + \acute{u}_i, \qquad v_i = \overline{v_i} + \acute{v}_i \qquad w_i = \overline{w_i} + \acute{w}_i$$

Where: $\overline{u_i}$ *and* $\acute{u}_i$ are the mean and fluctuating velocity components in x direction.

And also for pressure $p = \overline{p} + \acute{p}$.

By substituting this expression of the flow variables into the instantaneous continuity and momentum equations and taking a time (or ensemble) average and dropping the overbar on the mean velocity, yields the ensemble-averaged momentum equations. They can be written in Cartesian form as:

$$\frac{\partial \rho}{\partial t} + \frac{\partial}{\partial x_i}(\rho u_i) = 0$$

$$\frac{\partial}{\partial t}(\rho u_i) + \frac{\partial}{\partial x_j}(\rho u_i u_j) =$$

$$-\frac{\partial p}{\partial x_i} + \frac{\partial}{\partial x_j}\left[\mu\left(\frac{\partial u_i}{\partial x_j} + \frac{\partial u_j}{\partial x_i} - \frac{2}{3}\delta_{ij}\frac{\partial u_l}{\partial x_l}\right)\right] + \frac{\partial}{\partial x_j}(-\rho\overline{u_i' u_j'})$$

These two equations are called Reynolds-averaged Navier-Stokes (RANS) equations. They have the same general form as the instantaneous Navier-Stokes equations, with the velocities and other solution variables now representing ensemble-averaged (or time-averaged) values.

But there is Additional term now appear that represent the effects of turbulence. This term called Reynolds stresses ($-\rho\overline{u_i' u_j'}$), it must be modeled in order to close the equation.

RANS Models have two categories according to how the Reynolds Stress term is calculated.

- Reynolds Stress Models (RSM)
- Eddy viscosity models (EVM)

3.2.2.1 Reynolds Stress Models (RSM).

- In this category, Reynolds stress components are derived by averaging the products of velocity fluctuations and Navier-Stokes equations. A turbulent dissipation rate equation is also needed.

- RSM is most suitable for highly anisotropic, three dimensional flows where EVMs perform poorly (as will be mentioned). The computational cost is higher.
- Currently RSMs do not always provide indisputably superior performance over EVMs.

3.2.2.2 Eddy viscosity models (EVM).

- It is the most widely used turbulence models for CFD. this approach use Boussinesq hypothesis which relate the Reynolds stresses to the mean velocity gradients:

$$-\rho\overline{u_i'u_j'} = \mu_t\left(\frac{\partial u_i}{\partial x_j}+\frac{\partial u_j}{\partial x_i}\right)-\frac{2}{3}\left(\rho k+\mu_t\frac{\partial u_i}{\partial x_i}\right)\delta_{ij}$$

Where: μt: the effective turbulent viscosity, K: turbulence kinetic energy

$$k=0.5*\left(\overline{u'^2}+\overline{v'^2}+\overline{w'^2}\right)$$

EVM models:

- **Spalart-Allmaras model**

Spalart-Allmaras is a one equation, low-cost RANS model solving a transport equation for a modified eddy viscosity

– When in modified form, the eddy viscosity is easy to resolve near the wall

• Mainly intended for aerodynamic/turbomachinery applications with mild separation, such as supersonic/transonic flows over airfoils, boundary-layer flows.

• Embodies a relatively new class of one-equation models where it is not necessary to calculate a length scale related to the local shear layer thickness

• Designed specifically for aerospace applications involving wall-bounded flows

– Has been shown to give good results for boundary layers subjected to adverse pressure gradients.

– Gaining popularity for turbomachinery applications.

- **Standard K-Epsilon model (SKE)**

K-E family models are two equations models.

The Standard K-Epsilon model (SKE) is the most widely-used engineering turbulence model for industrial applications

• Model parameters are calibrated by using data from a number of benchmark experiments such as pipe flow, flat plate, etc.

• Robust and reasonably accurate for a wide range of applications

• Contains submodels for compressibility, buoyancy, combustion, etc.

• Turbulence energy k has its own transport equation:

$$\frac{\partial(\rho k)}{\partial t}+\frac{\partial(\rho \bar{u}_i k)}{\partial x_i}=-\rho\overline{u_i' u_j'}\frac{\partial \bar{u}_i}{\partial x_i}-\rho\varepsilon+\frac{\partial}{\partial x_i}\left[\left(\mu+\frac{\mu_t}{\sigma_k}\right)\frac{\partial k}{\partial x_i}\right]$$

• The dissipation rate, ε, is entirely modeled phenomenologically (not derived) as follows:

$$\frac{\partial(\rho\varepsilon)}{\partial t}+\frac{\partial(\rho u_i \varepsilon)}{\partial x_i}=\frac{\partial}{\partial x_j}\left[\left(\mu+\frac{\mu_t}{\sigma_\varepsilon}\right)\frac{\partial \varepsilon}{\partial x_j}\right]+C_{1\varepsilon}P_k\frac{\varepsilon}{k}-C_{2\varepsilon}\rho\frac{\varepsilon^2}{k}$$

• Dimensionally, the dissipation rate is related to *k* and a turbulence length scale:

$$\varepsilon \sim \frac{k^{3/2}}{L_t}$$

• Together ε with the *k* equation, eddy viscosity can be expressed as:

$$\mu_t=\rho C_\mu L_t\sqrt{k} \quad = \rho C_\mu\frac{k^2}{\varepsilon}$$

- limitations of the SKE model:

• Performs poorly for flows with larger pressure gradient, strong separation, high swirling component and large streamline curvature.

• Inaccurate prediction of the spreading rate of round jets.

• Production of *k* is excessive (unphysical) in regions with large strain rate (for example, near a stagnation point), resulting in very inaccurate model predictions.

- **Realizable k–ε (RKE) model:**

• Dissipation rate (ε) equation is derived from the mean-square vorticity fluctuation, which is fundamentally different from the SKE.

• Several realizability conditions are enforced for Reynolds stresses.

• Also have its own equations like SKE.

• Benefits:

− Accurately predicts the spreading rate of both planar and round jets

− Also likely to provide superior performance compared with the standard k-epsilon model for flows involving rotation, boundary layers under strong adverse pressure gradients, separation, and recirculation

- **RNG k–ε (RNG) model:**

• Constants in the k–ε equations are derived analytically using renormalization group theory, instead of empirically from benchmark experimental data.

• Dissipation rate equation is modified.

• Performs better than SKE for more complex shear flows, and flows with high strain rates, swirl, and separation

- **Standard k–ω (SKW):**

• Robust low-Reynolds-number (LRN) formulation down to the viscous sublayer.

• Several sub-models/options of k–ω: for compressibility effects, transitional flows and shear-flow corrections.

• Improved behavior under adverse pressure gradient.

• SKW is more sensitive to free-stream conditions.

• Most widely adopted in the aerospace and turbomachinery communities.

- **Shear Stress Transport k–ω (SSTKW) model:**

• The SST k–ω model uses a blending function to gradually transition from the standard k–ω model near the wall to a high-Reynolds-number version of the k–ε model in the outer portion of the boundary layer.

• Contains a modified turbulent viscosity formulation to account for the transport effects of the principal turbulent shear stress.

• SST model generally gives accurate prediction of the onset and the size of separation under adverse pressure gradient

Limitations and weakness of eddy viscosity models:

• Linear algebraic stress-strain relationship results in poor performance where stress transport is important, including non-equilibrium flows, separating and reattaching flows, etc.

• Inability to account for extra strain due to streamline curvature, rotation, and highly skewed flows, etc.

• Poor performance where turbulence is highly anisotropic (e.g., in flows where normal stresses play an important role) and/or 3D effects are present.

Note:

There are many techniques (submodels) used under each of the EVM models for modelling near-wall flow such as: solving viscous sublayer, standard wall function, enhanced wall treatment, scalable wall function…etc.

3.3 The present model

3.3.1 Model building

The model was built on **ANSYS 14.0** workbench and the solver used is **Fluent** and its own design modeler was used for geometry building.

2D model was selected because of the symmetry of the sluice cross section in the lateral direction. The 2D model gave the advantage of building real dimensions model (without scaling) due to low number of cells and so low computational cost.

The model geometry sketched according to low level sluice drawings provided by the contractor (3D As-built), it is Max. 84.71m long in X direction, Max.11.15m high in Y direction.

The effort concentrated on the targeted areas (seal area), and due to the fact that the pressure head is the only condition available as an explicit boundary condition at the outlet, the outlet divided into small (*named selection*) parts to guarantee an acceptable gradation of outlet pressure and avoid inserting part of the river into the model. The surface body of 2D model is shown in figure 2.2 and 2.3 below.

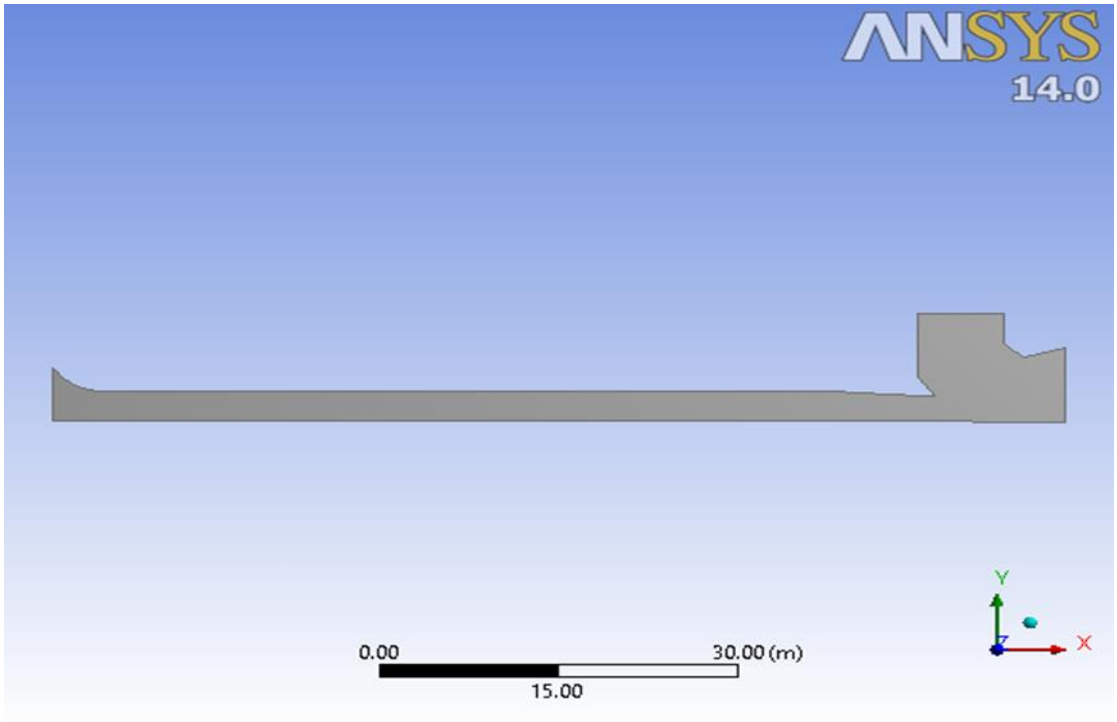

Figure 2.2: L.L.S model, 2D surface body

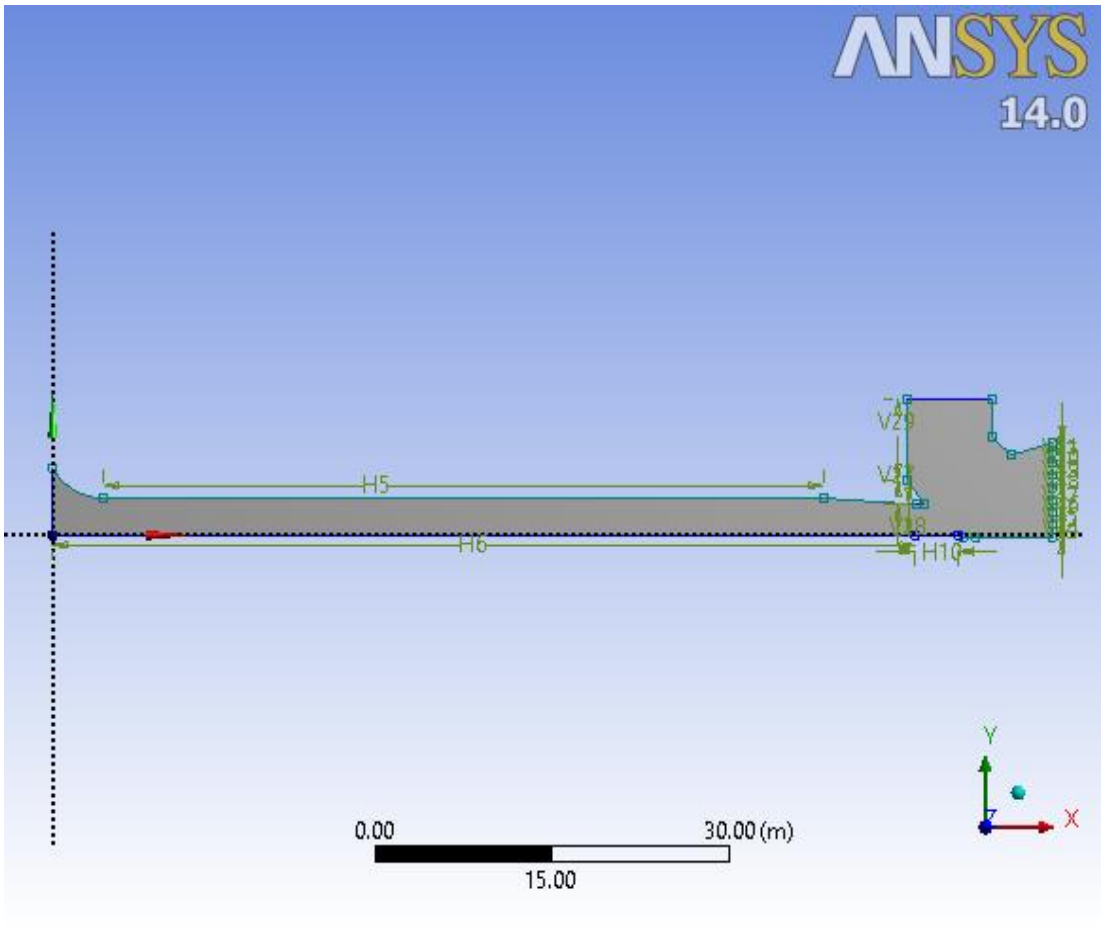

Figure 2.3: sketch of L.L.S 2D model

3.3.2 Cell mesh

- The dominant cell area is 5cm^2 and mesh sizing used to reduce this value to 1cm^2 on the targeted areas
- Total number of cell 147552 cell.
- More mesh techniques and refinement not applicable due to computational cost, this result in low mesh quality in some areas as shown in figure 2.5 below.

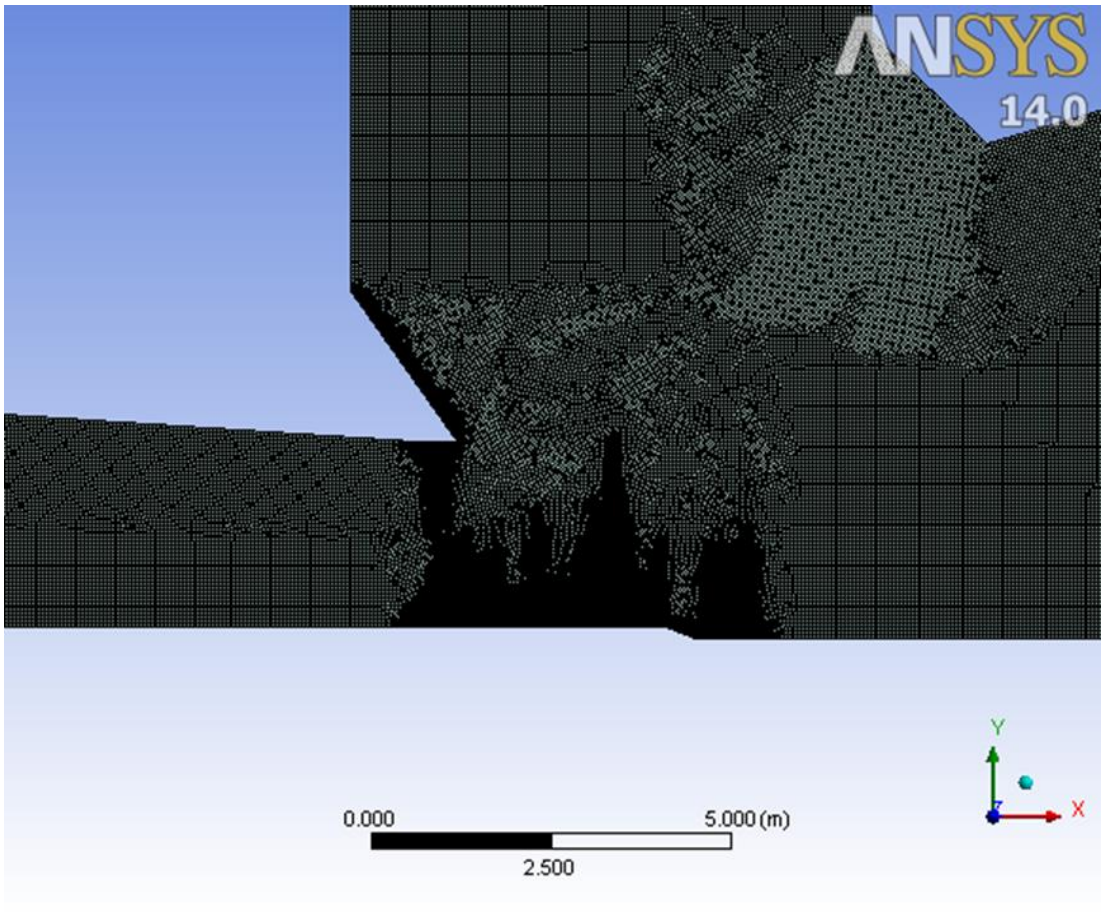

Figure 2.4: cell mesh of L.L.S model

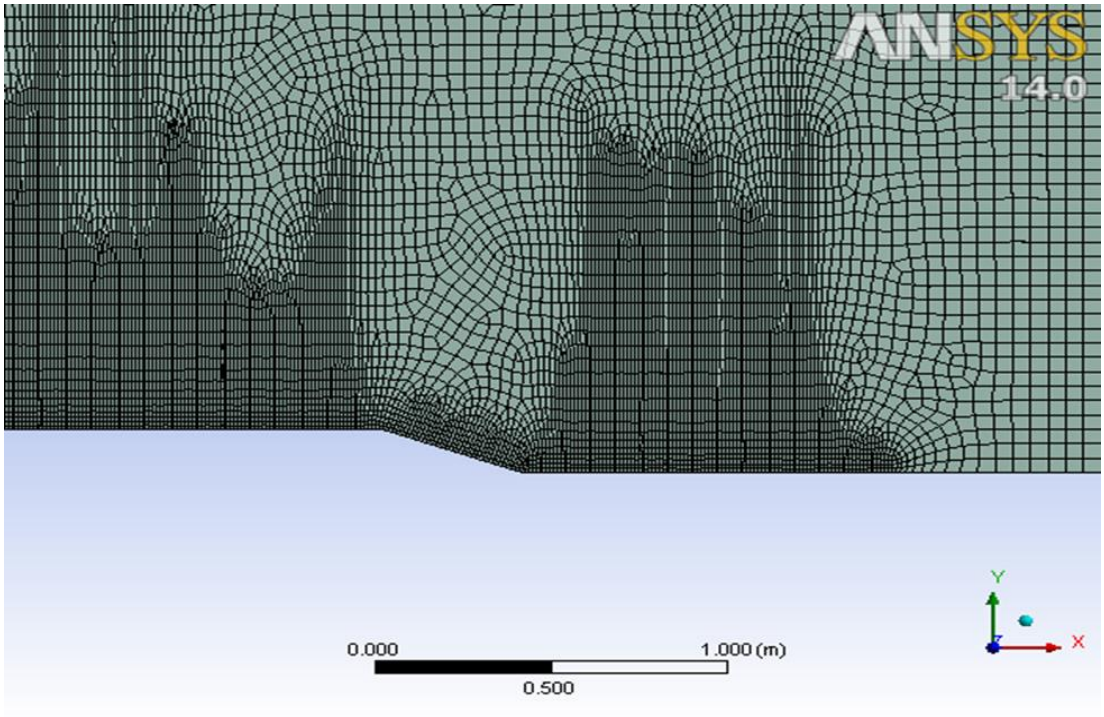

Figure 2.5: cell mesh of the lower seal area

3.3.3 Turbulence model & boundary conditions

- The boundaries is inlet, outlet, outlet vent and walls, upstream level 290m AMSL, downstream level 254m AMSL, so the **boundary conditions** is:
  - 46m H_2O gage pressure at inlet, taken at 1m above the bottom of sluice passageway.
  - 8 sections outlet gage pressure, gradual increment from bottom up according to downstream pressure over outlet section level (from 242.85m – 250.5m AMSL).
  - Zero gage pressure at outlet vent.
  - No slip for all walls.
- **The turbulent model** used: realizable K-E (RKE), standard wall function.
  - Many types of turbulent models tried before selecting the above appropriate model.
- Solution method: second order discretization for momentum &turbulence, standard discretization for pressure.
- Number of solution iteration 3000, its residual chart shown in figure 2.6 below.

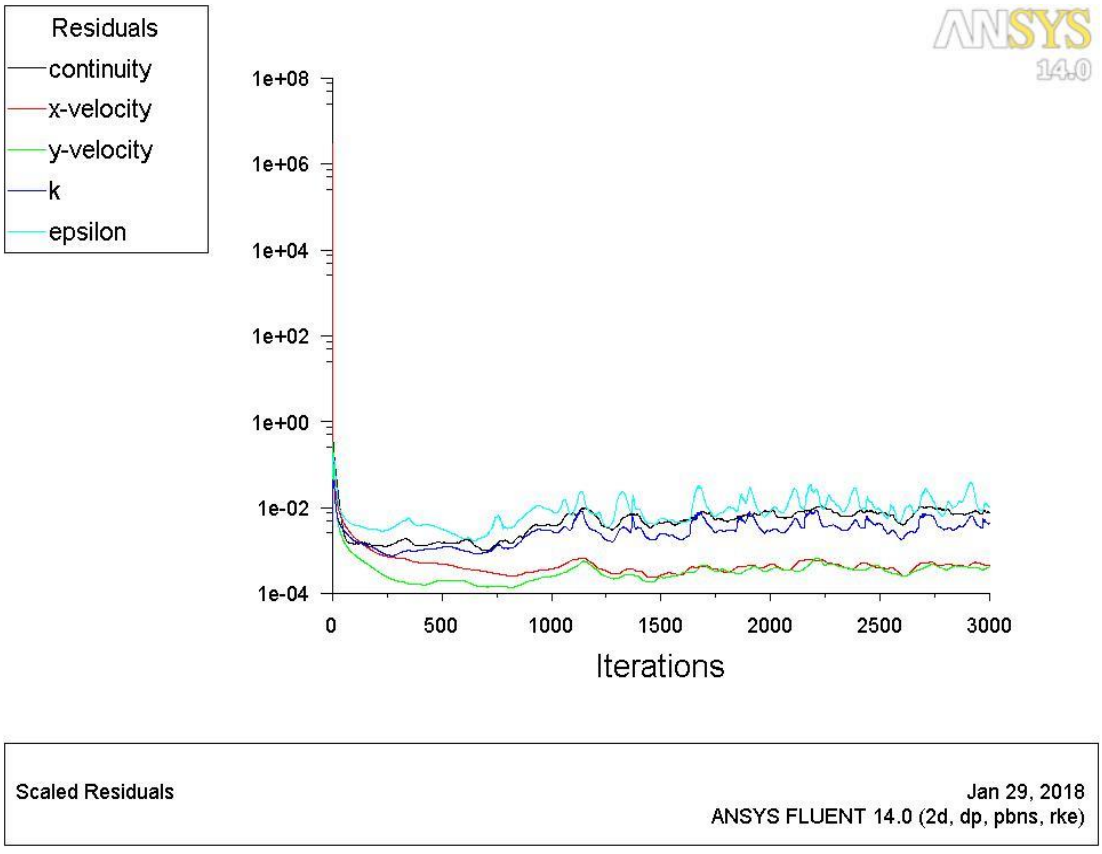

Figure 2.6 solution residual

CHAPTER IV

RESULTS DISCUSSION & VALIDATION

In this chapter it will be the discussion of the information's extracted from the built software model, to conclude the results and ensure its validity by comparing some of them against measured and physical information's.

4.1 Results validation.

As mentioned, the validation process will be ensured in two ways as below.

4.1.1 Validation by measured values.

Because of the fact that the only available conditions at boundaries of the model are static pressure at the inlet and outlet, this give the advantage of using flow velocity and discharge as a tester for results validity.

The average discharge through sluice passageway:

- Software model discharge v=13.8m/s→1.03Mm^3/Hr.(refer fig.4.1)
- Instruments measured discharge (average of many days) =1.07Mm^3/Hr. (more than 96% conformity)

4.1.2 Validation by physical observation.

The other validation test executed by using cavitation phenomenon observed in the simulation.

At the area close to the beginning (upstream side) of lower seal, at the edge of sloped surface, there is a velocity acceleration (max.32.4m/s) leading to pressure drop (min. -291300Pa), followed by sharply incremented pressure as shown in the figure 4.5, 4.6, which means possibility of **cavitation** in the area of pressure drop (weak point to which the imploded voids directed). The direction of imploded voids expected to be opposite to flow direction.

Cavitation pitting position at the edge and its direction opposite to flow could be observed on the pictures taken at the sluice in the yearly check. Refer pictures No. 1, 2, and 3 on pictures appendix.

4.2 Results discussion.

In this section the saved pictures of contours and streamlines will be discussed to extract a useful informations about flow behaviors and then conclude the final results.

- X direction average velocity through passage way = 23.8 m/s →1.03Mm^3/hr. which close to the instruments measured value (1.07Mm^3/hr.). refer figure 4.1

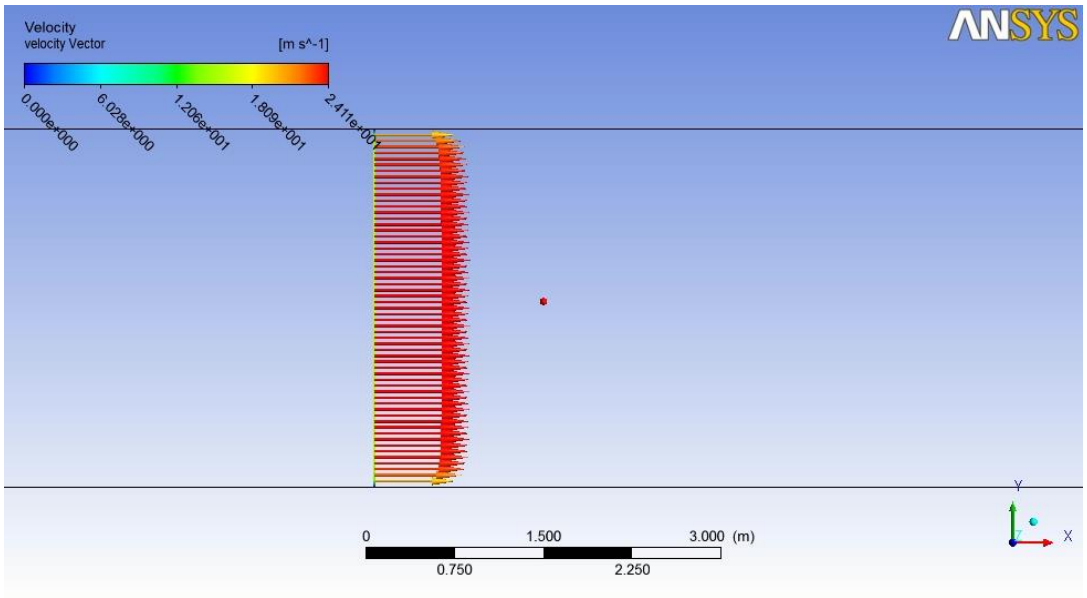

Figure 4.1 water flow velocity through L.L.S passageway

- High total pressure in the area of lower seal (> 2.5 bar) →high shear force due to **pressure drag** on the rubber seal, (figure 4.2). From the shape of damage of the rubber seal, it is mainly due to shear force. Refer pictures 4, 5 on pictures appendix.

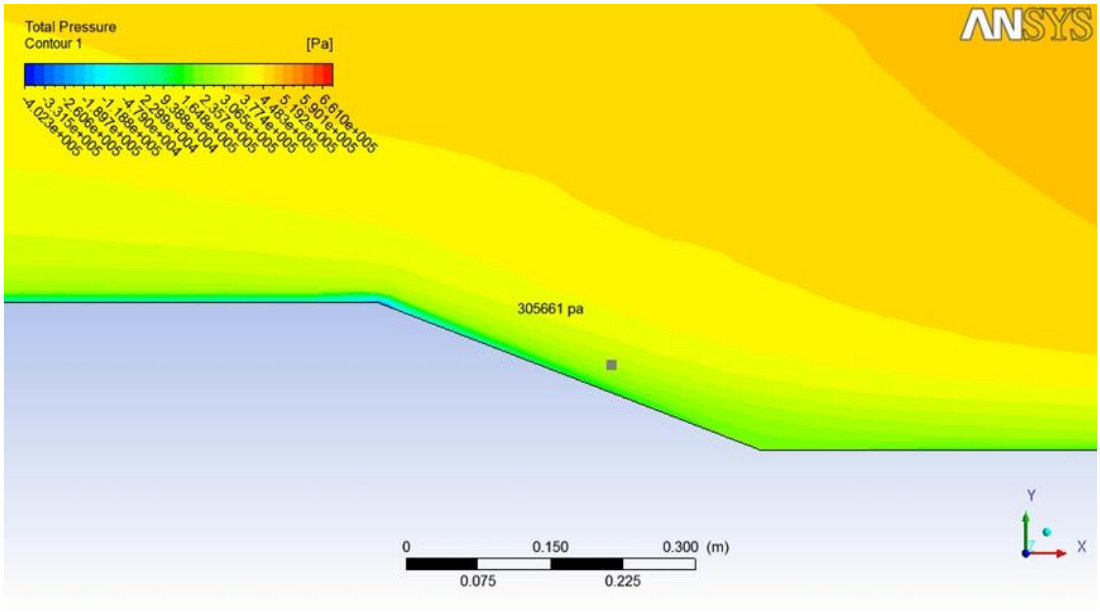

Figure 4.2 total pressure in the lower seal area

- High velocity (>13.5m/s) at the area of lower seal → high shear force due to the high **skin drag** (figure 4.3, 4.4). This is the second component of the shear force and represents the major component of the shear force applied on the seal.

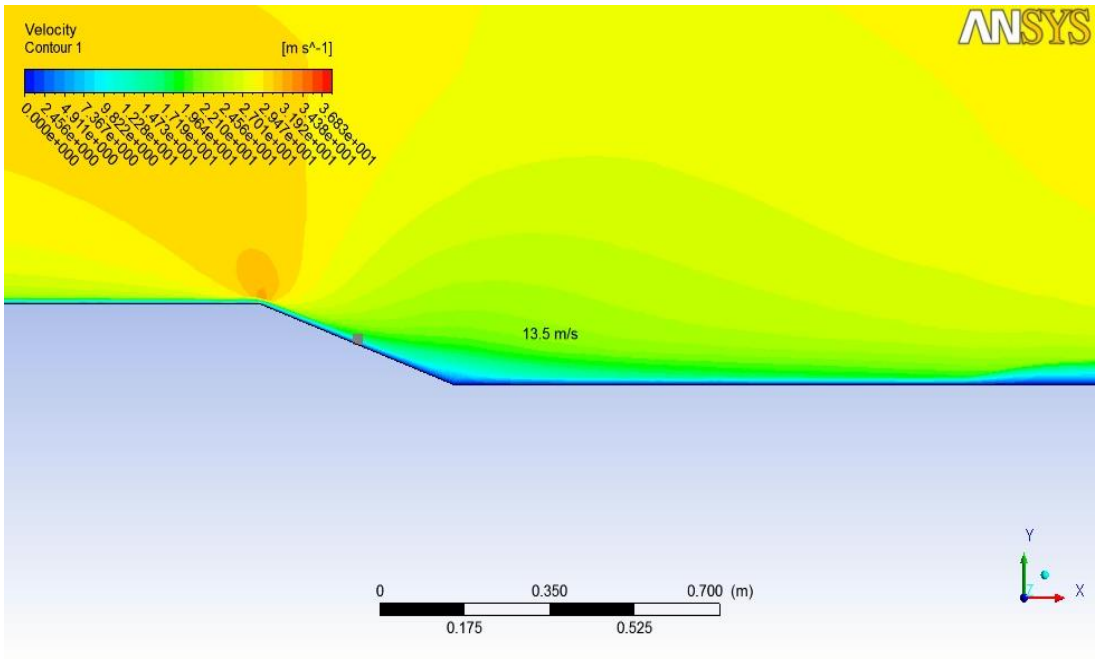

Figure 4.3 flow velocity at lower seal area

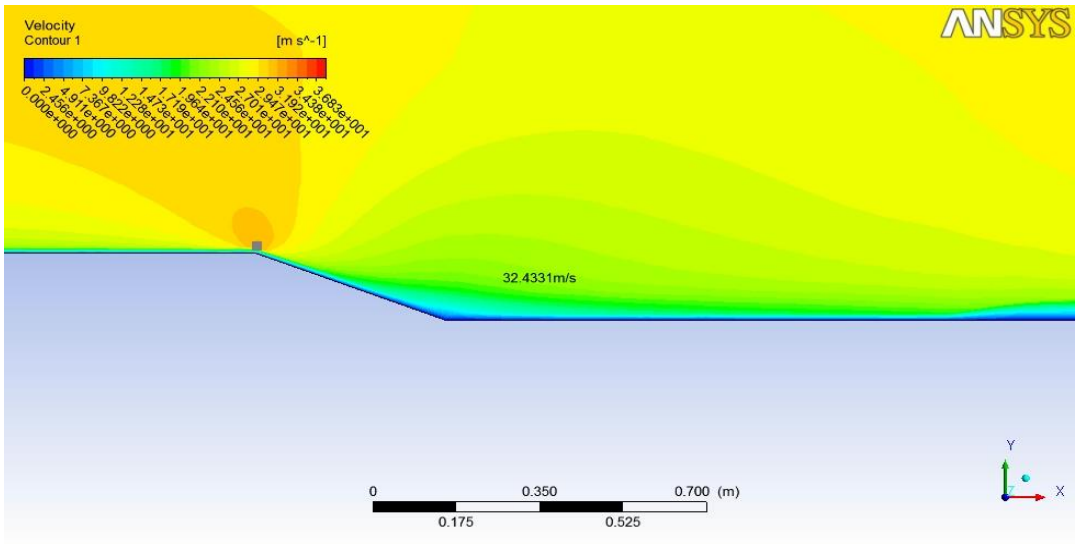

Figure 4.4 flow velocity of lower seal area

- In the area close to the beginning (upstream side) of the lower seal there is a pressure drop (about - 291300Pa gage pressure) followed by incrementing pressure (figure 4.5, 4.6), which means possibility of **cavitation** in the area of pressure drop (weak point to which the imploded voids directed. Refer pictures 1, 2, 3 on pictures appendix.

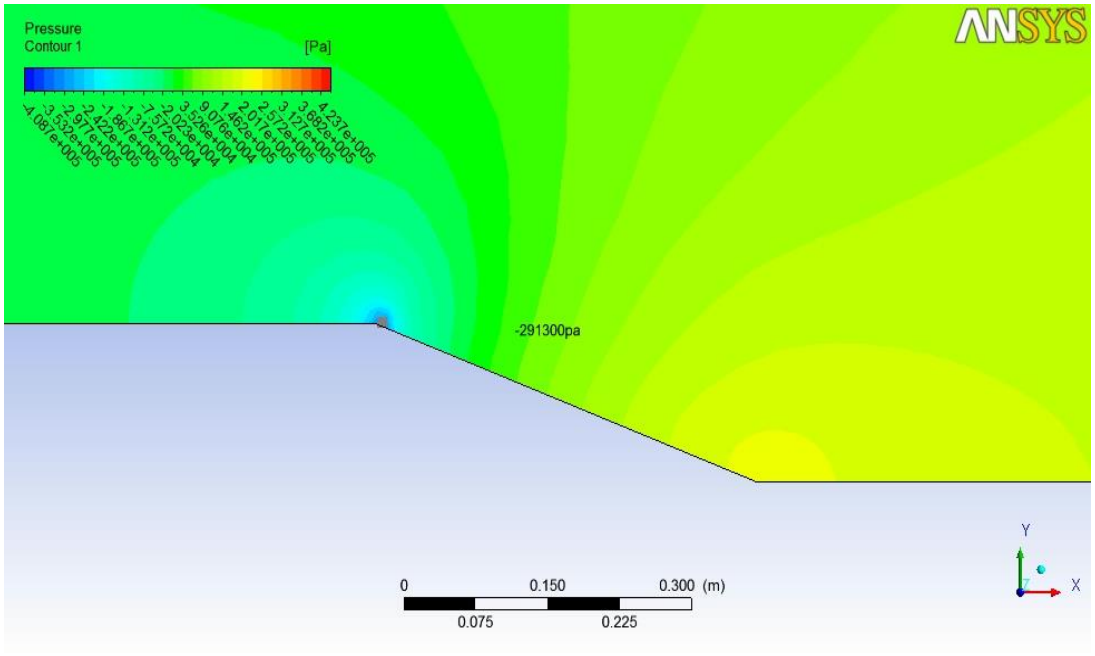

Figure 4.5 pressure drop, (cavitation) area

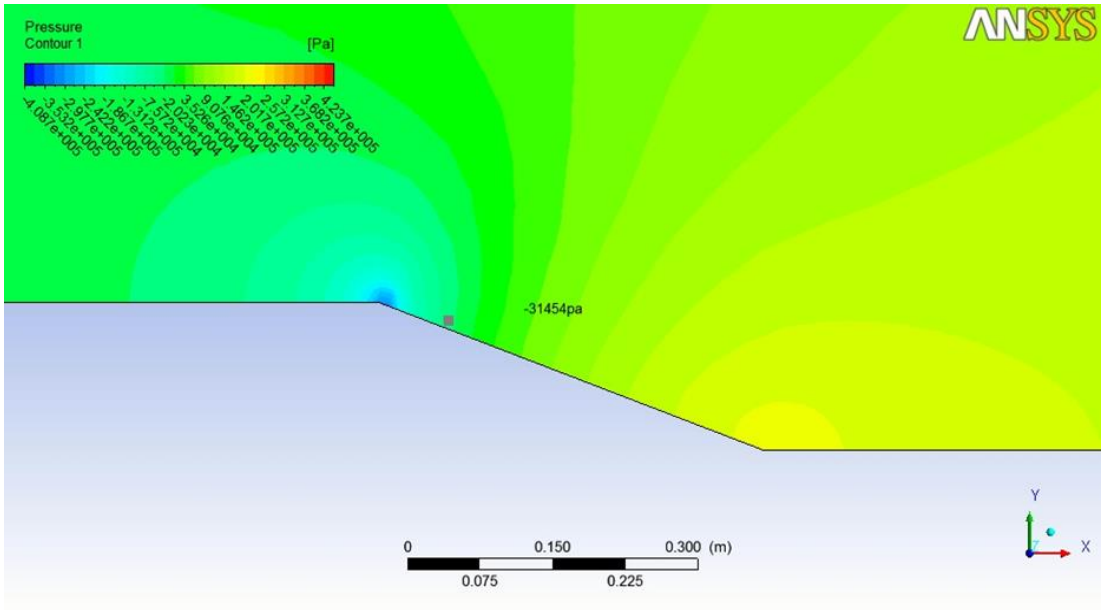

Figure 4.6 pressure drop, (cavitation) area

- A concrete jump with random estimated dimensions was inserted to the model geometry in front of (upstream side) the lower seal area to reduce the magnitude of total pressure and velocity and to shift cavitation area as shown in figure 4.7, 4.8, 4.9 below.

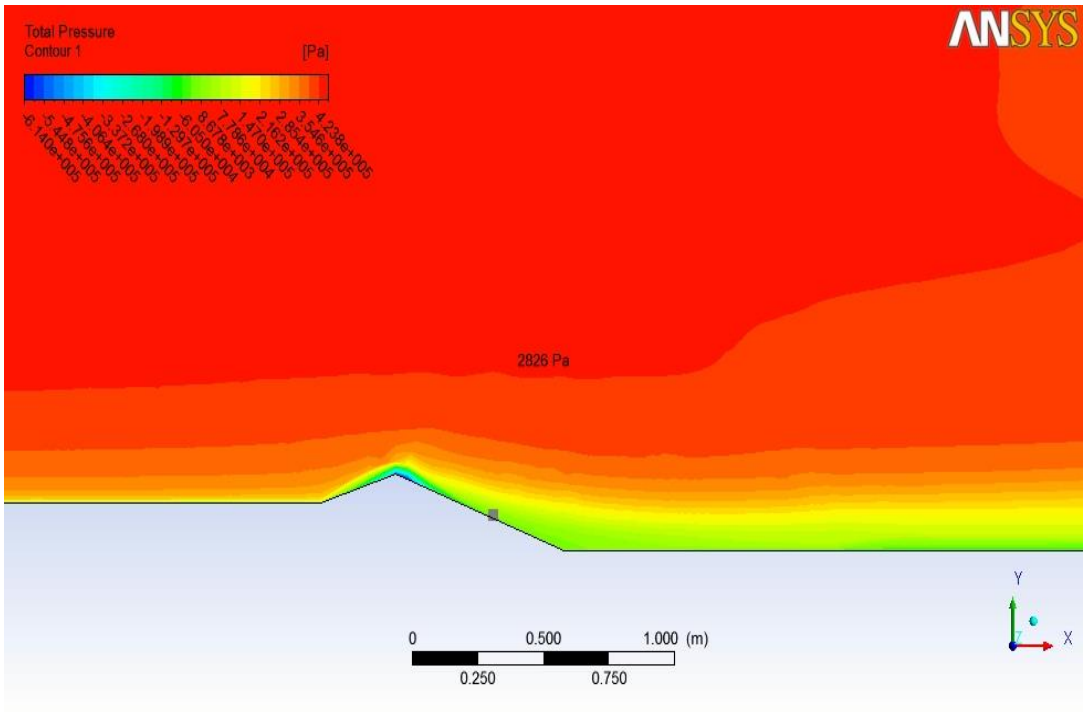

Figure 4.7 concrete jump, seal area pressure

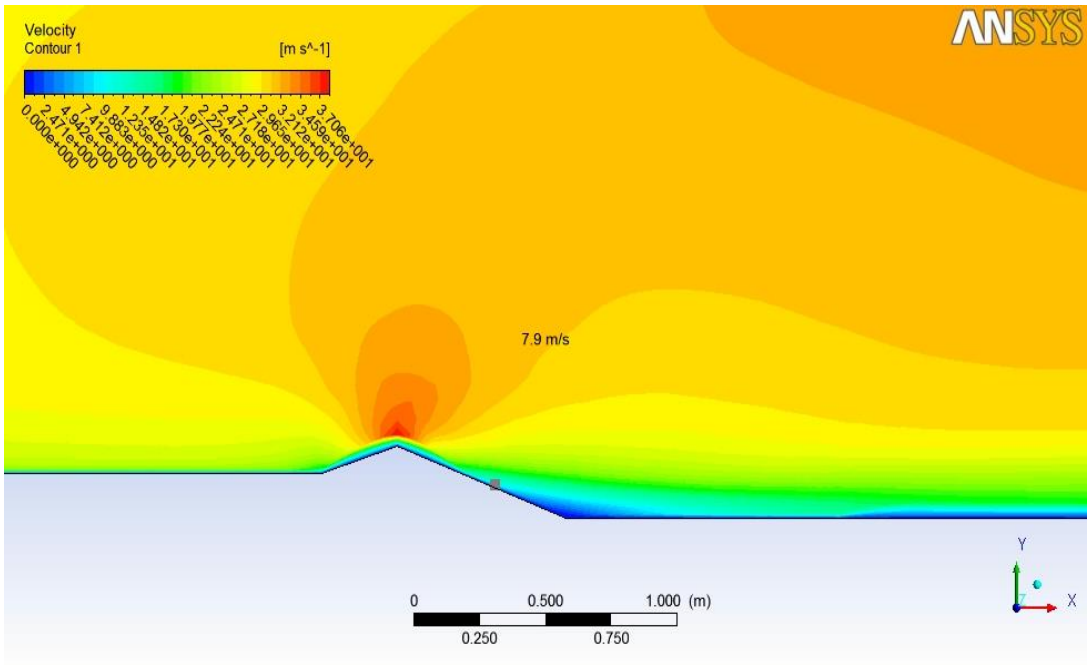

Figure 4.8 concrete jump seal area velocity

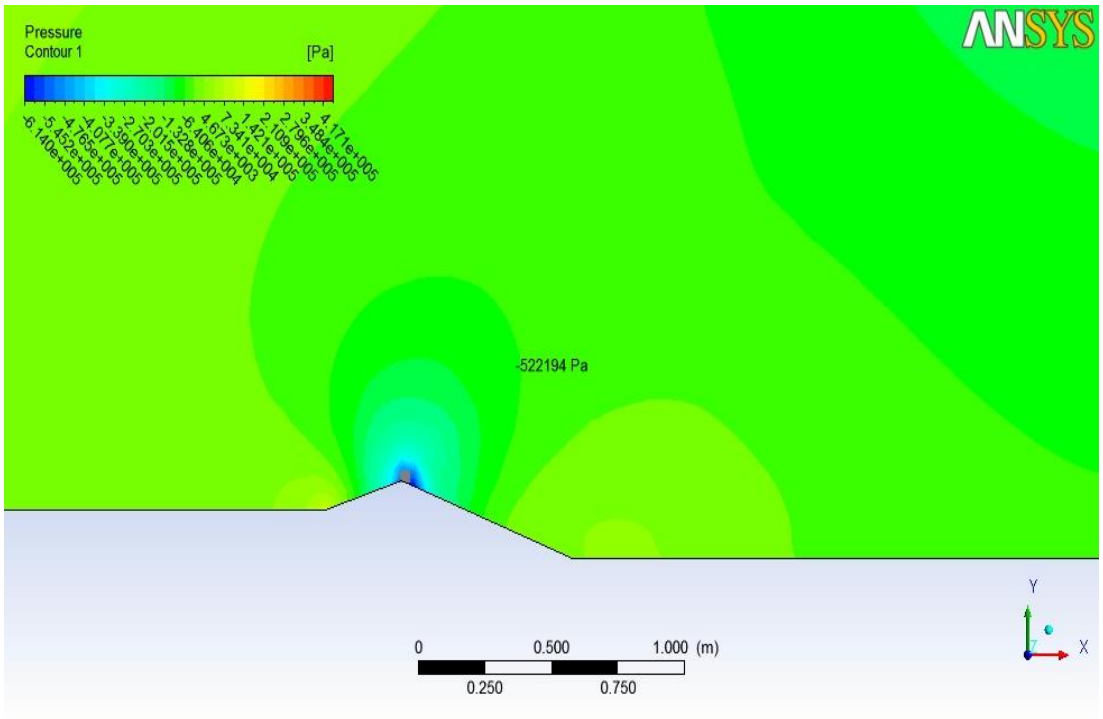

Figure 4.9 concrete jump, pressure drop

- **On the upper seal area:** there is a fluid stagnation and low positive static pressure in the area of upper seal (figure 4.10, 4.11), so no influence on the seal except one sluice seal damage which made by the gate due to inflatable seal applying while gate operation . refer picture No.6

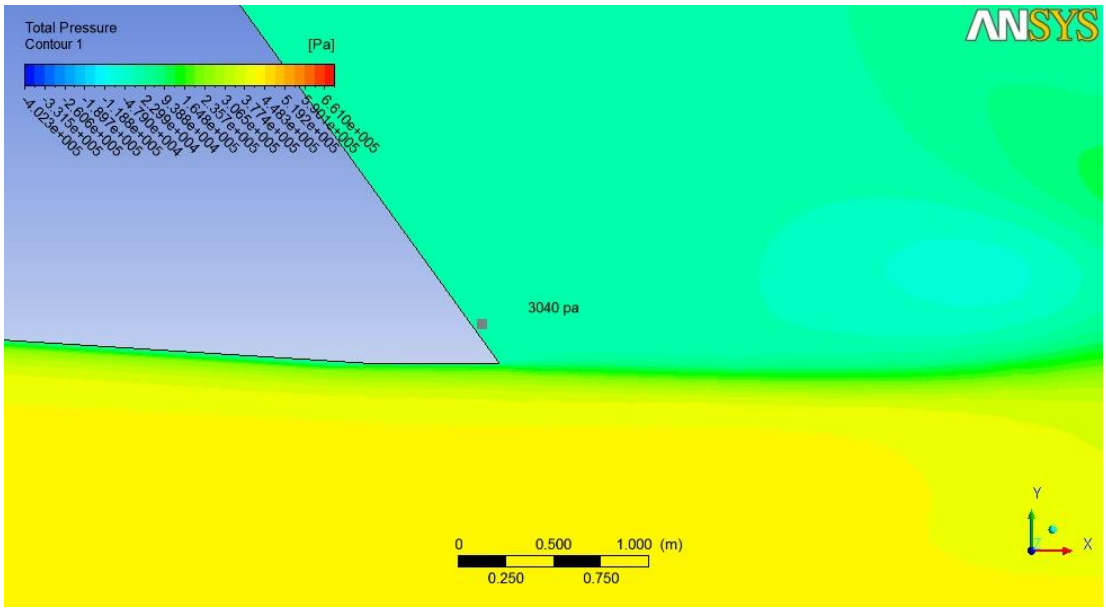

Figure 4.10 upper seal pressure contour

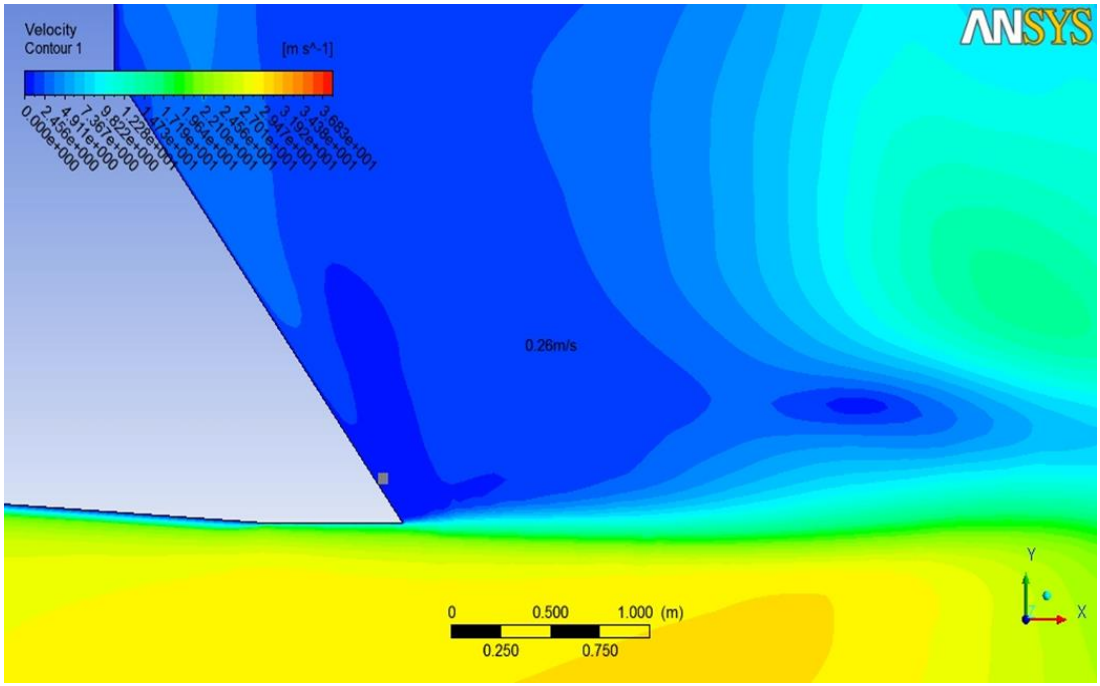

Figure 4.11 upper seal pressure contour

- **Turbulence intensity** not concentrated on the upper or lower seal (figure 4.12), so it has no effect on the seal except the area above the upper seal may be affected by turbulence. Refer picture No. 7

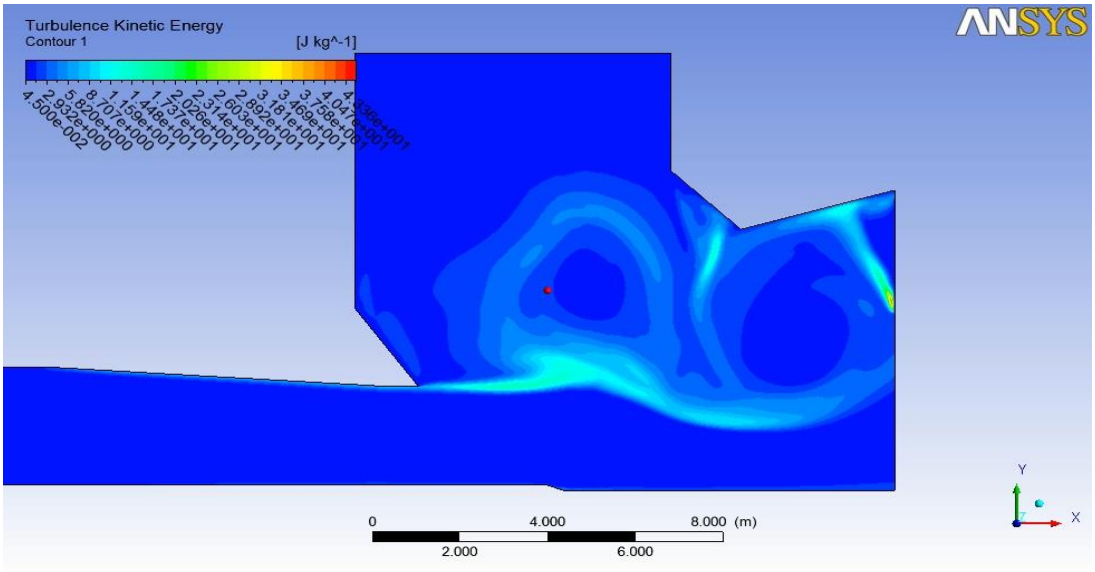

Figure 4.12 turbulence intensity

- The two **sides seal** not included in the model because it require 3D model, but from the taken pictures, it is clear that the mechanism of damage is different from that of the lower seal. The rubber seal was in good conditions and not affected, but the bolts of the clamp have untightened and the clamp was washed out. (refer pictures 8, 9, 10).

CHAPTER V

CONCLUSION & RECOMMENDATIONS

5.1 results conclusion

The work of the present study has done and its final results must be concluded. But before jumping to the results it must be gone back and refer to the assumptions taken before and while model building.

The problem of water sealing may be due to weak fixing of rubber seal, but the assumption is that this approach was excluded and the study focused only on hydrodynamic approach, so there is additional approach need to take its portion of study and analysis.

The second assumption is that the water flow was assumed and described as steady flow, this assumption has a significant effect in software model building. But from the discussion of results in previous chapter, the main cause of damage is the force applied on the rubber seal, and by referring to Bernoulli equation introduced in chapter two, it clarify that the transient stage represents an additional forces or amplify the shear force applied on the seal due to large increasing in the velocity and dynamic pressure while gate opening or closing. So there is no inconsistency in the results.

The results conclusion can be written as the following points:

- The results is reliably valid.
- The damages of lower rubber seal is due to shear force (combination of skin and pressure drag) as a result of high velocity and total pressure.
- The transient stage while gate opening and closing maximize the shear force.
- The upper seal not affected obviously by the flow.
- Building a concrete jump in front of lower seal area can reduce the undesirable velocity and pressure (force) on the seal.
- The two side seals damages not included in the model because it require 3D model, but from the damage style it looks like as it has been via different mechanism.

5.2 recommendations

Taking in the consideration the above results and to contribute on solution of the problem of water sealing in L.L.S, it is recommended to take the following points in consideration:

1. Rebuilding the software model in 3D to study the status of two sides seal.
2. Re-implementing the study with better computational resources.
3. Building a concrete jump in front of lower seal area with thoughtful and accurate dimensions to avoid any bad side effects of geometry change.
4. Confirmation of no partial opening.
5. For assurance take in consideration the other route of solution (seal fixture).

REFERENCES

Hama, D, 2017. Cavitation phenomenon research for different flow conditions. World scientific news

د. محمد هاشم صديق ، ميكانيكا الموائع، دار جامعة الخرطوم للنشر، ٢٠٠٦

Shankar Subramanian, R. 29/April/2018. The equation of conservation of mass. www.Scribed.com/document.

Perio, J, Sherwin, S, 2005. Finite difference, finite element and finite volume methods for partial differential equations. Springer.

SINOHYDRO CORPORATION, 2005. Operation and maintenance manual - outlet portal of low level sluice main Radial gate. Merowe dam project implementation unit

Chapter10. Modeling Turbulence, 29/April/ 2018. www.afs.enea.it/fluent/Public/Fluent/-Doc/PDF

ANSYS customer training material, 2010. Introduction to ANSYS FLUENT, lec6 (Turbulence modeling), release 13. ANSYS.

College of Water Resources and Hydropower, State Key Laboratory of Water. Resources and Hydropower Engineering Science, 2011. Program of the Hydraulic and Flow-Induced Vibration, Model Test for Low-Level Sluices Working Gate, Merowe Dam Project. China: Wuhan University.

شركة كهرباء سد مروي ادارة الصيانه الميكانيكيه. نتائج إجتماعات ممرات الإطماء فى الفترة من ٢٣ الى ٢٦ نوفمبر ٢٠١٢

Appendix A

Pictures

Picture No. 1

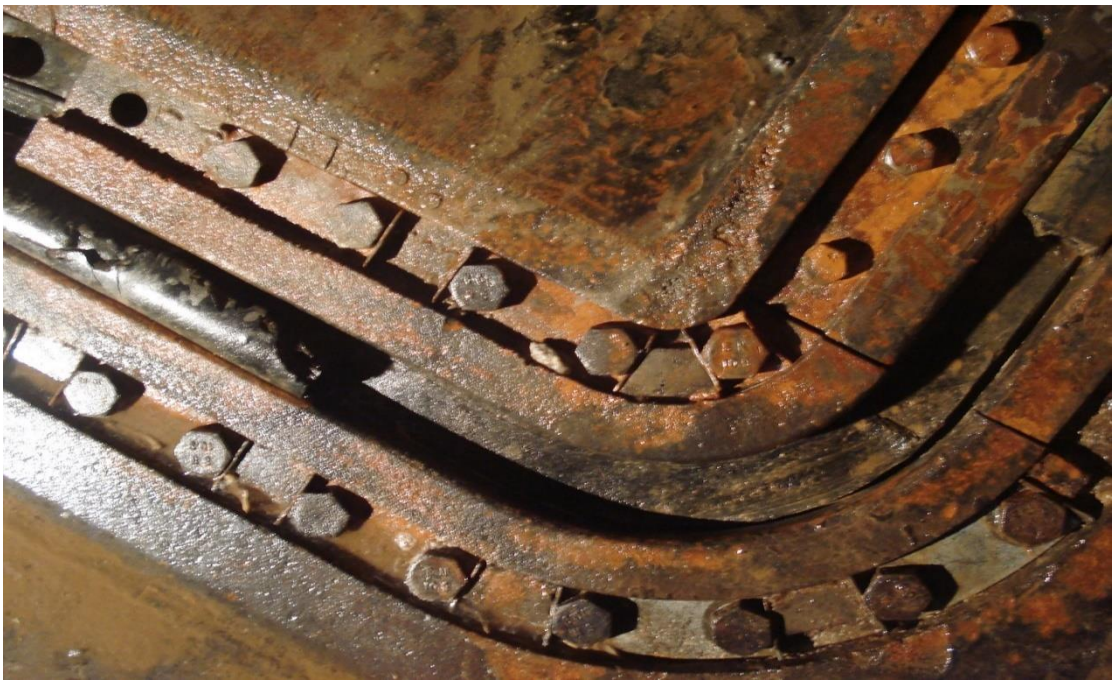

Picture No. 2

Picture No. 3

Picture No. 4

Picture No. 5

Picture No. 6

Picture No. 7

Picture No. 8

Picture N0. 9

Picture No. 10